



Mean-field theory of superradiant phase transition in complex networks

Andrei Yu. Bazhenov , Dmitriy V. Tsarev , and Alexander P. Alodjants

National Research University for Information Technology, Mechanics and Optics (ITMO), St. Petersburg 197101, Russia



(Received 22 July 2020; revised 9 March 2021; accepted 28 May 2021; published 21 June 2021)

In this work we consider a superradiant phase transition problem for the Dicke-Ising model, which generalizes the Dicke and Ising models for annealed complex networks presuming spin-spin interaction. The model accounts for the interaction between a spin-1/2 (two-level) system and external classical (magnetic) and quantized (transverse) fields. We examine regular, random, and scale-free network structures characterized by the δ function, random (Poisson), and power-law exponent [$p(k) \propto k^{-\gamma}$] degree distributions, respectively. To describe paramagnetic (PM)-ferromagnetic (FM) and superradiant (SR) phase transitions we introduce two order parameters: the total weighted spin z component and the normalized transverse field amplitude, which correspond to the spontaneous magnetization in z and x directions, respectively. For the regular networks and vanishing external field we demonstrate that these phase transitions generally represent prerequisites for the crossover from a disordered spin state to the ordered one inherent to the FM and/or SR phase. Due to the interplay between the spin interaction and the finite-size effects in networks we elucidate novel features of the SR state in the presence of the PM-FM phase transition. In particular, we show that the critical temperature may be high enough and essentially depends on parameters which characterize statistical properties of the network structure. For the scale-free networks we demonstrate that the network architecture, characterized by the particular value of γ , plays a key role in the SR phase transition problem. Within the anomalous regime scale-free networks possess a strong effective spin-spin interaction supporting fully ordered FM state, which is practically nonsensitive to variations of the quantum transverse field or moderate classical magnetic field. In a scale-free regime the networks exhibit vanishing of the collective spin component in z direction with increasing γ accompanied by establishing spontaneous magnetization in the transverse field. The SR phase transition occurs in the presence of some FM state. We establish the conditions for the network parameters, classical and quantum field features to obtain a quantum phase transition in the spin system when the critical temperature approaches zero.

DOI: [10.1103/PhysRevE.103.062309](https://doi.org/10.1103/PhysRevE.103.062309)

I. INTRODUCTION

Currently, complex networks evoke an enormously increasing interest among the scientific community performing advanced studies at the boundary of physics, social and cognitive sciences, and applied mathematics [1–3]. In particular, these studies aim to investigate complex processes in social networks and on the Internet [4,5], in living systems integrated within biological networks [6], designing new (quantum) materials with complex topology and structure [7–9], developing communications and information network technologies including quantum networks [10,11]. Complex networks and, especially, (hyper)network structures are inherent to modern cognitive science and current brain activity research [12].

Despite the fact complex network studies are largely interdisciplinary, in many cases they are based on the models and approaches of statistical physics, which allow obtaining sufficiently clear dependencies for nontrivial processes in various network structures [13]. The Ising model is one that has been well established in such works [14]. In particular, an Ising-type model was proposed to explain the opinion formation and social impact [15]. This model was recently revised in the framework of collective emotions [16], social cohesion, and structural balance [17].

The Ising model for scale-free networks possessing arbitrary degree distribution was comprehensively studied by Leone *et al.* [18] by the replica method. The random transverse Ising model on the complex networks with a scale-free degree distribution was examined in the framework of superconductor-insulator phase transitions [19]. Notably, the annealed network approximation was explored in Ref. [20] to characterize scale-free networks.

It seems important to stress that the Ising model allows depicting complex (scale-free) network models exhibiting a second-order phase transition and Bose-Einstein condensation (BEC) phenomenon [21]. In contrast to random networks, the scale-free, so-called Barabási-Albert (BA), model considers a preferential link connection during network growing. This situation can be established in the framework of the Ising annealed network approach that possesses a power-law distribution of degrees [22,23]. Some peculiarities of a ferromagnetic (FM) phase transition and criticality in such a model, which occurs for large but finite-size network systems, represent a primary interest in Refs. [24,25]. The mean-field approach to the Ising model on networks with a degree distribution is discussed in Refs. [14]. In recent research [26] Krishnan *et al.* examined the mean-field approach based on the effective long-range interacting homogeneous Ising model

to describe the Ising model on a BA network. By means of Monte Carlo simulations and analytical approach to BA network it was shown that such a model is reasonable in a low-temperature domain and above the critical temperature. However, the role of degree exponent γ for scale-free networks was not discussed in Ref. [26].

Noteworthy, the critical behavior of the Ising model manifests due to the spin-spin interaction. The interaction of spins with a classical (constant transverse) external field is typically studied in the framework of the so-called transverse Ising model, cf. Ref. [27].

In this work we focus on the problem when the transverse field represents some variable which allows for a second quantization procedure. In this case, spin systems may be represented as two-level oscillators like natural or artificial two-level atoms [28], quantum dots, etc, which interact with the quantized field in the framework of the Dicke model. This model presumes a so-called superradiant (SR) second-order phase transition, and has been long known in quantum optics domain [29–32]. In particular, the SR phase transition evokes the establishment of some certain (nonzero) spontaneous polarization, that occurs in a thermodynamically equilibrium ensemble of two-level oscillators interacting with the quantized field.

To the present, the SR phase transition has been predicted and observed with atomic ensembles [33–35], exciton polaritons in semiconductor microstructures [36], superconductor circuits [37,38], solids [39], and extended star graphs [40]. The evidence of the SR state in such experiments is usually achieved by means of cavity exploiting that enables to enhance a photon lifetime [9,41,42]. Moreover, the quantized light interaction with various two-level system ensembles enables high- (up to room) temperature phase transitions, cf. Refs. [34,36]. Such a feature of the Dicke-Ising model that we offer in this work may be useful for the problem of obtaining high-temperature BEC, which is now a hot topic of research in statistical physics and material science, cf. Refs. [43,44].

In particular, two different regimes are relevant to be distinguished when the SR phase transition occurs in the system. First, we speak about the zero chemical potential limit when we can describe the total system in the framework of the canonical ensemble approach. In this case, the ensemble of two-level oscillators and photonic system are thermodynamically equilibrium closed subsystems [29–32]. Second, the grand canonical approach presumes a nonzero chemical potential when photons and spins (or two-level systems) can form coupled states (dressed states, polaritons), which possess the SR phase transition [34,36]. In other words, at nonzero chemical potential we can speak about BEC of low branch polaritons that occurs in the system in the presence of appropriate trapping potential [43–45]. In this work we restrict ourselves by canonical ensemble approach to the network spin-1/2 system, which interacts with classical and quantized fields.

Recently, the SR phase transition has been discussed in Refs. [46,47] in the framework of the so-called Dicke-Ising model for the material systems exhibiting spin-spin interaction. In particular, in Refs. [46,47] it is demonstrated that such systems permit a first-order phase transition depending on the

character of spin-spin interaction. Some important applications in quantum metrology are also found [48].

In Ref. [16] we established the Dicke-like model for the collective decision-making problem that exhibits the second-order phase transition that occurs in heterogeneous information-oriented communities interacting with information field. In particular, we showed that the system demonstrates social polarization and lasing phenomena for certain parameters (density of excitations, temperature). In this sense our model bridges the gap between the laserlike models described in Refs. [49,50] and current studies on opinion formation which involve echo-chamber effects in social network communities [51,52]. However, the network topology and (Ising-like) coupling between agents eventually play a vital role for various socially oriented statistical models, see Refs. [4,5,22,23,51–53] and cf. Ref. [16].

Surprisingly, the phase transitions problem for the Dicke-Ising model specified for complex networks has not been studied yet at all; this work aims to investigate it. We are going to elucidate the role of particular network characteristics, such as node degree, degree exponent (for scale-free networks) in the SR phase transition that activates the network structure. In particular, an important task of this work is to show how the establishment of the superradiant transverse quantum field affects the spin ordering in the orthogonal z direction.

The paper is arranged as follows. In Sec. II we offer the Dicke-Ising model that exploits the annealed complex networks approach. The equations for the order parameters are derived in the framework of variational (thermodynamic) approach. Specifically, we explore the mean-field approach, which is familiar in quantum optics, cf. Refs. [30,36,42]. This approach deals with coherent state ansatz for quantized field, which presumes neglect of spin-spin and spin-quantized field correlations. However, as we show, it allows to account degree correlations in the network structure. In Sec. III we discuss the complex network parameters that play an essential role in the phase transition problem. Moreover, we examine regular, random, and scale-free networks. The scale-free networks are examined in the anomalous, scale-free, and random regimes, which are characterized by different values of degree exponent, cf. Refs. [4,5]. The phase transition problem for the complex networks in the presence of the quantized transverse field is comprehensively studied in Secs. IV and V. We investigate various limits in respect of the classical magnetic field, degree exponent, statistical properties of network degree. In Sec. IV we examine regular networks characterized by a constant spin-spin interaction strength. In this case, we obtain simple analytical treatments describing the SR phase transition in the presence of FM and/or paramagnetic (PM) states for both low- and high-temperature limits. Section V presents the solution of the phase transition problem in the scale-free and random networks, which possess strong spin-spin interaction depending on the network architecture. In addition, we study the quantum phase transition problem for the complex networks attained in the zero-temperature limit. Some specific problems connected with the SR phase transition in the low-temperature limit with regular networks are given in Appendix. In Sec. VI the results obtained are summarized.

II. THE DICKE-ISING MODEL FOR COMPLEX NETWORKS

Let us consider the ensemble of N spin-1/2 (or two-level) systems (particles), which randomly occupy N nodes of a complex network. We represent the complex network as a graph with nontrivial (specific) properties, resulting from its topology, degree distribution, and other characteristics, see Refs. [1,2,5]. The spins, which are placed in the nodes of the graph, are supposed to interact with classical (local) magnetic field h_i and the quantized (transverse) field. We describe the transverse field by means of annihilation (a) and creation (a^\dagger) operators. The total Hamiltonian of the model reads

$$H = - \sum_{ij} J_{ij} \sigma_i^z \sigma_j^z - \frac{1}{2} \sum_i h_i \sigma_i^z + \omega_a a^\dagger a - \frac{1}{2\sqrt{N}} \sum_i \chi_i \sigma_i^x (a + a^\dagger), \quad (1)$$

where σ_i^z and σ_i^x , $i = 1, \dots, N$, characterize the i th particle spin components in z and x directions, respectively. The sum is performed over the graph vertices with certain adjacency matrix A_{ij} proportional to J_{ij} , it stores the information about the graph structure: matrix element $A_{ij} = 1$ if two vertices are linked and $A_{ij} = 0$ otherwise.

First two terms in Eq. (1) describe the Ising model, while the last terms are inherent to the Dicke model. The Dicke part of H in Eq. (1) is responsible for the spin interaction with the quantized transverse (“photonic”) field possessing energy $\hbar\omega_a$ (in this work for simplicity we put the Planck and Boltzmann constants $\hbar = 1$, $k_B = 1$). Parameter χ_i in (1) characterizes the coupling of spin x component, σ_i^x , with the quantum transverse field in the so-called dipole approximation. Below we restrict ourselves to a homogeneous problem when $h_i = h$ and $\chi_i = \chi$ for any i .

Notably, (1) describes the Husimi-Temperley-Curie-Weiss model that belongs to the transverse Ising model if in (1) we assume $\chi_i(a + a^\dagger)/\sqrt{N} \rightarrow \epsilon_i$, i.e., in the limit of the fixed, constant, classical transverse field, cf. Ref. [27]. However, in this work average photon number $N_{\text{ph}} \equiv \langle a^\dagger a \rangle$ accumulated in the transverse field is a variable that relates to the order parameter of the SR phase transition.

We are more interested in the annealed network approach that presumes a weighted, fully connected graph model. This network is dynamically rewired. Two nodes i and j are connected with probability p_{ij} that looks like, cf. Ref. [19]

$$p_{ij} = P(A_{ij} = 1) = k_i k_j / N \langle k \rangle, \quad (2)$$

where A_{ij} is an element of the adjacency matrix, k_i is i th node degree taken from distribution $p(k)$. In (2) $\langle k \rangle = \frac{1}{N} \sum_i k_i$ is an average degree.

Noteworthy, the annealed network approach is valid for $p_{ij} \ll 1$ and for large-enough N , cf. Ref. [54]. We recast parameter J_{ij} that indicates the coupling between the nodes in Eq. (1) through probability p_{ij} as $J_{ij} = J p_{ij}$, where J is a constant.

Thus, the strength of two spins interaction J_{ij} is a variable parameter and depends on particular network characteristics; it is greater for two pairs of nodes with the highest k coefficient.

The properties of the system described by Eq. (1) may be determined by means of two order parameters. The first order parameter, S_z , is a collective weighted spin component defined as

$$S_z = \frac{1}{N \langle k \rangle} \sum_i k_i \sigma_i^z. \quad (3)$$

The second one, λ , is a normalized mean transverse field amplitude

$$\lambda = \frac{|\alpha|}{\sqrt{N}} = \sqrt{\frac{N_{\text{ph}}}{N}}, \quad (4)$$

where we use Glauber coherent state basis $|\alpha\rangle$ for the quantized transverse field that contains $N_{\text{ph}} = \langle \alpha | a^\dagger a | \alpha \rangle = |\alpha|^2$ photons on average.

The physical meaning of Eqs. (2) and (3) becomes more evident if we introduce local effective magnetic field $H_{\text{eff},i} \equiv 2 \sum_j J_{ij} \sigma_j^z + h$ that acts on the i th node spin. Combining the first two terms of (1) with (2) for $H_{\text{eff},i}$ we obtain

$$H_{\text{eff},i} = 2Jk_i S_z + h. \quad (5)$$

The first term in $H_{\text{eff},i}$ depends both on spin-spin interaction strength J and collective weighted spin component S_z . The network system peculiarities become unimportant in the limit of strong classical field $h \gg J$. On the other hand, for $h = 0$ spin ordering completely depends on local properties of the i th node connectivity.

We can take into account the cumulative role of locally acting effective magnetic fields $H_{\text{eff},i}$ by total effective field $H_{\text{eff}} = \frac{1}{N} \sum_i H_{\text{eff},i}$ that looks like

$$H_{\text{eff}} = 2J \langle k \rangle S_z + h. \quad (6)$$

From (6) it is clear that spin-dependent peculiarities, which are determined by H_{eff} , depend on the network topology encoded in average degree $\langle k \rangle$. Thus, the limit of zero classical field $h = 0$ is of primary interest to elucidate these peculiarities.

To determine order parameters (3) and (4) for some temperature $T \equiv 1/\beta$, we use a variational (thermodynamic) approach, see, e.g., Ref. [29]. We exploit partition function $Z = \text{Tr}(e^{-\beta H})$. The mean-field approach that we use in this work (cf. Ref. [30]), presumes exploring factorized total state ansatz $|\Psi\rangle$ and representing it as $|\Psi\rangle = |\alpha\rangle |s_1 \dots s_N\rangle$, where $|s_1 \dots s_N\rangle$ defines an N -spin state. Strictly speaking, for the partition function we have:

$$Z = \frac{1}{\pi} \sum_{s_i} \int d^2\alpha \langle \Psi | e^{-\beta H} | \Psi \rangle. \quad (7)$$

Assuming $\int \frac{d^2\alpha}{\pi} = N \int_0^\infty d\lambda^2$ for the transverse coherent photonic state and performing integration in (7), for partition function Z we obtain

$$Z = N \int d\lambda^2 e^{-\beta N \omega_a \lambda^2} e^{-\beta J N \langle k \rangle S_z^2} \times \prod_i 2 \cosh \left[\frac{\beta}{2} \sqrt{(4Jk_i S_z + h)^2 + 4\chi^2 \lambda^2} \right]. \quad (8)$$

Evaluating the integral in Eq. (8) by Laplace method after some calculations we obtain the mean-field equations for

collective spin S_z , Eq. (9a), and average transverse field λ , Eq. (9b), respectively:

$$S_z = \frac{1}{N\langle k \rangle} \sum_i k_i \frac{\Theta S_z k_i + H}{\sqrt{(\Theta S_z k_i + H)^2 + 4\lambda^2}} \times \tanh \left[\frac{\beta}{2} \sqrt{(\Theta S_z k_i + H)^2 + 4\lambda^2} \right], \quad (9a)$$

$$\lambda \Omega_a = \lambda \frac{1}{N} \sum_i \frac{\tanh \left[\frac{\beta}{2} \sqrt{(\Theta S_z k_i + H)^2 + 4\lambda^2} \right]}{\sqrt{(\Theta S_z k_i + H)^2 + 4\lambda^2}}. \quad (9b)$$

In Eqs. (9) we introduce the normalized dimensionless parameters as

$$\Theta = 4J/\chi; \quad H = h/\chi; \quad \Omega_a = \omega_a/\chi; \quad \beta\chi \mapsto \beta. \quad (10)$$

Noteworthy, the latter expression in (10) implies dimensionless temperature $T/\chi \mapsto T$ that we use below.

Since the number of nodes is large enough, $N \gg 1$, we are interested in network structures, which admit continuous degree distribution $p(k)$. The transition from the discrete to continuous version of Eq. (9) may be performed by replacing $\frac{1}{N} \sum_i \dots \rightarrow \int_{k_{\min}}^{k_{\max}} \dots p(k) dk$, where k_{\min} and k_{\max} are the minimal and maximal values of node degree k . In this case, from (9) we can obtain:

$$S_z = \int_{k_{\min}}^{k_{\max}} \frac{k p(k)}{\langle k \rangle} \frac{(\Theta S_z k + H)}{\Gamma} \tanh \left[\frac{\beta}{2} \Gamma \right] dk, \quad (11a)$$

$$\lambda \Omega_a = \lambda \int_{k_{\min}}^{k_{\max}} p(k) \frac{\tanh \left[\frac{\beta}{2} \Gamma \right]}{\Gamma} dk, \quad (11b)$$

where we made denotation $\Gamma \equiv \sqrt{(\Theta S_z k + H)^2 + 4\lambda^2}$.

Let us briefly describe possible phase states, which may appear in the system determined by Eqs. (11).

Equation (11a) is inherent to the FM-PM phase transition. For nonvanishing (constant) λ this equation may be connected with the superconductor-insulator phase transition problem, cf. Ref. [19].

Equation (11b) looks as a gap equation in the Bardeen-Cooper-Schrieffer theory of superconductivity, cf. Ref. [55]. In our case, Eq. (11b) governs superradiant properties determined by another order parameter λ . Physically, λ is responsible for the temperature-dependent energy gap (Rabi splitting) that occurs due to the interaction of the two-level system with the quantized field in the framework of the Dicke model, cf. Refs. [29–32,34]. This work aims to find joint solutions of Eqs. (11), which correspond to the states with $S_z \neq 0$, $\lambda \neq 0$.

The phase transitions that we consider can be established by means of spontaneous magnetizations along x and z axes, which are defined as $m_{x,z} = \text{Tr}[\sigma_i^{x,z} e^{-\beta H}]/Z$, see, e.g., Ref. [27]. Magnetization in z direction coincides with the collective weighted z component of the spin, i.e., $m_z = S_z$. Another magnetization component m_x is proportional to the order parameter λ . This magnetization is similar to spontaneous polarization of two-level system that occurs in the framework of conventional Dicke model, cf. [16].

The nonsuperradiant (non-SR), normal phase corresponds to the trivial solution of Eq. (11b) with $\lambda = 0$ and is characterized by the absence of transverse magnetization, $m_x = 0$.

In this limit only Eq. (11a) solution is responsible for the phase transition from the PM state ($S_z = 0$) to the FM state ($S_z \neq 0$) in the network system. Notably, this limit for the Dicke-Ising model may be recognized completely in the Ising model framework, where the phase transition appears only due to finite-size effects, cf. Refs. [24,25].

The SR phase corresponds to nonzero (positive) λ that characterizes the activation (excitation) of the network nodes possessing spontaneous transverse magnetization $m_x \neq 0$. The Dicke model is well discussed previously in the framework of SR phase transition [29–32]. The model considers noninteracting particles, i.e., we should suppose $J = 0$ in (1). In this limit Eqs. (11) are essentially simplified, and the effects occurring due to network structure properties are completely ignored.

Thus, the transition from some disordered state with $m_z = m_x = 0$ to the ordered one with $m_z \neq 0$, and/or $m_x \neq 0$ appearing for $J \neq 0$ represents a primary interest for this work.

III. NETWORK ARCHITECTURES

In this work we consider the regular, random, and scale-free networks with the properties determined by various distribution functions $p(k)$. In particular, we characterize the networks by means of the first ($\langle k \rangle$) and second ($\langle k^2 \rangle$) moments for the degree distribution, which are defined as:

$$\langle k^m \rangle = \int_{k_{\min}}^{k_{\max}} k^m p(k) dk, \quad m = 1, 2. \quad (12)$$

Below we exploit the parameter

$$\zeta = \frac{\langle k^2 \rangle}{\langle k \rangle} \quad (13)$$

that determines the basic statistical properties of the chosen network.

The typical networks considered in this work are shown in Fig. 1. Spin-1/2 particles are placed in the network nodes. Figures 1(a)–1(c) represents randomly allocated spin-up and spin-down configuration particles with the average total spin equal to zero. The configuration of the network obeys a certain distribution function, $p(k)$, established in Fig. 1(d). In particular, the networks in Figs. 1(a)–1(c) demonstrate the case where the numbers of spin-up and spin-down particles are equal.

First, we examine a regular network, see Fig. 1(a). It can be established as a network with Delta-function degree distribution $p(k) = \delta(k - k_0)$ and a certain positive constant degree of nodes $k = k_0$. From definitions (12) and (13) we immediately obtain $\langle k^m \rangle = k_0^m$ ($m = 1, 2$) and $\zeta = k_0$, respectively.

Physically, the regular network implies constant interaction strength Θk_0 for an arbitrary pair of spins. It is maximal for the complete graph with N nodes and $k_0 = N - 1$.

Second, we discuss a scale-free network in the framework of the SR phase transition problem. In particular, we examine the degree distribution obeying the power law

$$p(k) = \frac{(\gamma - 1) k_{\min}^{\gamma-1}}{k^\gamma}, \quad (14)$$

where γ is a degree exponent and k_{\min} is the smallest degree for which Eq. (14) holds. In this work we examine the region $1 < \gamma \leq 4$ which covers the anomalous ($1 < \gamma <$

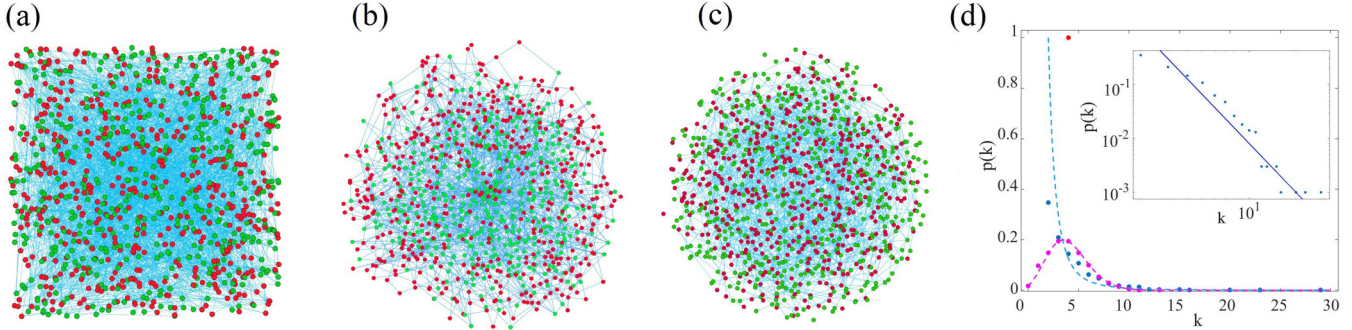


FIG. 1. (a) Regular, (b) scale-free, (c) random networks and (d) the relevant degree distributions are plotted for $N = 1000$ and $\langle k \rangle = 4$. The red (green) nodes in (a)–(c) correspond to the “spin-up” (“spin-down”) states. The average magnetization is $S_z = 0$. The magenta (blue) curves represent Poisson (power-law) degree distribution in (d). Single (red) point characterizes the Delta-function distribution with $k_0 = 4$. The insert shows the degree distribution in a logarithmic scale for the scale-free (BA) network. Points sequences located in right corner in inset, indicate presence of hubs for BA network in (b).

2), scale-free ($2 < \gamma < 3$), and random ($\gamma > 3$) regimes, cf. Refs. [1,3]. The properties of scale-free networks possessing distribution (14) for $\gamma = 2$ and $\gamma = 3$, should be calculated separately. As an example, in Fig. 1(b) we plot the numerically generated scale-free, Barabási-Albert (BA), network with $\gamma = 3$.

The normalization condition for $p(k)$ is the following:

$$\int_{k_{\min}}^{+\infty} p(k)dk = 1. \tag{15}$$

An important feature of the scale-free network is the existence of hubs, which are clearly recognized by means of four points located in the right corner of the inset in Fig. 1(d). The largest hub is described by degree k_{\max} called a natural cutoff. The condition

$$\int_{k_{\max}}^{+\infty} p(k)dk = \frac{1}{N} \tag{16}$$

can be used if the network with N nodes possesses more than one node with $k > k_{\max}$. From Eqs. (14) and (16) we obtain $k_{\max} = k_{\min}N^{\frac{1}{\gamma-1}}$, cf. Ref. [3]. Notably, in the anomalous regime $k_{\max}/k_{\min} > N$.

In Table I we represent the analytical treatments for the scale-free network characteristics $\langle k \rangle$ and ζ in the limit of large N . The relevant dependence of $\langle k \rangle$ and ζ on degree exponent γ are presented in Fig. 2. As clearly seen, both characteristics increase in the anomalous region. It is worth noting that within this region of parameter γ , the effective magnetic field in Eqs. (5) and (6) may be enormously large

even in the limit of $H = 0$. In other words, the networks in anomalous regime support strong spin-spin interaction.

On the other hand, in the scale-free and random regions $\langle k \rangle$ and ζ vanish. As we show below, these features of the scale-free network parameters play a crucial role in the SR phase transition problem.

Third, we consider a random (Poissonian) network model that consists of N nodes and M edges, see Fig. 1(c), cf. Refs. [1,3]. Each edge is included in the network with probability w , which is independent from other edges. For a very large N and finite $\langle k \rangle = (N - 1)w \simeq Nw$ it is possible to consider the Poisson degree distribution $p(k)$; it is shown in Fig. 1(d) by the magenda curve:

$$p(k) = \frac{\langle k \rangle^k e^{-\langle k \rangle}}{k!}. \tag{17}$$

From Eqs. (12), (13), and (17) we deduce that $\zeta = 1 + \langle k \rangle$ in this case. Noteworthy, the mean-field approach is valid for the Ising model above the critical point $\langle k \rangle = 1$, when a large cluster with size $N^{2/3}$ is formed [10].

The estimation of upper (k_{\max}) and lower (k_{\min}) natural cutoffs for random networks with the Poisson distribution (17) is discussed in Ref. [3]. In particular, we can infer the largest node degree k_{\max} of the random network from the numerical solution of $Ne^{-\langle k \rangle} \frac{\langle k \rangle^{k_{\max}+1}}{(k_{\max}+1)!} \approx 1$. This equation may be obtained from the discrete version of (16). As before we assume that in the random network there exists no more than one node with the degree higher than k_{\max} . Notably, hubs effectively disappear for the random network since the dependence of k_{\max} on N is practically negligible.

TABLE I. Behavior of average degree $\langle k \rangle$, ζ parameter, and critical number N_c for the scale-free network with degree distribution $p(k) \propto k^{-\gamma}$ for various values of degree exponent γ in the limit of large N . The parameters are specified in the text.

γ	$\langle k \rangle$	ζ	N_c
$\gamma > 1, \gamma \neq 2, \gamma \neq 3$	$k_{\min}^{\frac{\gamma-1}{2-\gamma}} (N^{\frac{2-\gamma}{\gamma-1}} - 1)$	$k_{\min}^{\frac{2-\gamma}{3-\gamma}} \frac{N^{\frac{3-\gamma}{\gamma-1}} - 1}{N^{\frac{2-\gamma}{\gamma-1}} - 1}$	$(\frac{2\langle k \rangle}{\Theta k_{\min}^2} \frac{3-\gamma}{\gamma-1} T_c + 1)^{\frac{\gamma-1}{3-\gamma}}$
2	$k_{\min} \ln(N)$	$\frac{k_{\min}}{\ln(N)} N$	$\frac{2\langle k \rangle}{\Theta k_{\min}^2} T_c$
3	$2k_{\min}$	$\frac{k_{\min}}{2} \ln(N)$	$e^{\frac{8T_c}{\Theta \langle k \rangle}}$

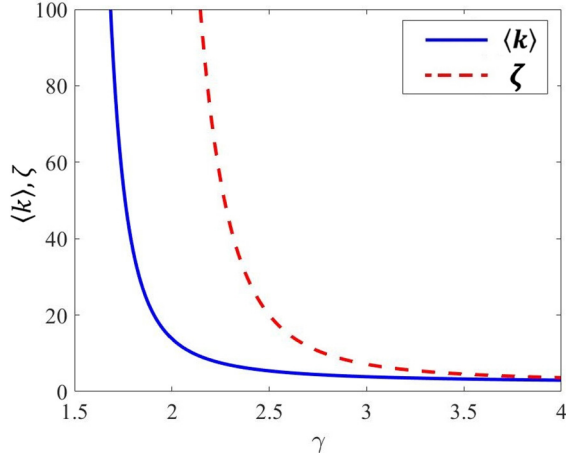


FIG. 2. Dependence of mean degree, $\langle k \rangle$, and ζ parameter on degree exponent γ for the scale-free network at $N = 1000$.

For the random networks, that we examine in this work, average degree $\langle k \rangle$ belongs to supercritical regime domain $1 < \langle k \rangle < \ln(N)$ that is relevant to a moderate number of nodes (we consider networks with $N = 1000$), cf. Ref. [3]. Physically, such networks possess isolated nodes, see Fig. 1(c). In this regime we can take $k_{\min} \geq 0$.

IV. PHASE TRANSITIONS IN REGULAR NETWORKS

Let us start from the regular network analysis that admits relatively simple analytical solutions of Eqs. (11). Equations (11) now can be represented as

$$S_z = \frac{\Theta k_0 S_z + H}{\Gamma_0} \tanh\left[\frac{\beta}{2} \Gamma_0\right], \quad (18a)$$

$$\Omega_a = \frac{\tanh\left[\frac{\beta}{2} \Gamma_0\right]}{\Gamma_0}, \quad (18b)$$

where $S_z = \frac{1}{N} \sum_i \sigma_i^z$ simply represents the additive (collective) spin z -component variable, cf. (3); $\Gamma_0 \equiv \Gamma(k = k_0) = \sqrt{(\Theta S_z k_0 + H)^2 + 4\lambda^2}$.

Combining together Eqs. (18a) and (18b) we can establish the necessary condition for the existence of the SR phase transition solution in the system.

In particular, the solution of (18b) (for FM phase, $S_z \simeq 1$) exists if the condition

$$(\varepsilon + \Omega_a H)^2 + 4\Omega_a^2 \lambda^2 \leq 1 \quad (19)$$

is fulfilled. In (19) we make denotation $\varepsilon = \Theta k_0 \Omega_a$.

When the considered system is very close to the fully ordered FM state, we represent the total spin component as $S_z \simeq 1 - \delta$, where δ is positive small perturbation ($\delta \ll 1$) to the ordered state. In this case Eqs. (19) and (18a) lead to the condition $2\Omega_a^2 \lambda^2 \leq \delta - 0.5\delta^2$. Notably, the fully ordered FM state with $S_z = 1$ may be obtained only in the limit of the absence of any perturbations ($\delta = 0$) that implies the absence of superradiance, $\lambda = 0$.

Our approach to the analysis of Eqs. (18) is as follows. First, we consider nonzero classical field H that implies some FM state for S_z . In this limit it is possible to examine conditions for the occurrence of the SR phase transition.

Second, we examine Eqs. (18) considering vanishing classical field $H \rightarrow 0$, which admits the phase transition from the collective spin disordered state to some ordered one, cf. Ref. [27].

A. Ferromagnetic SR phase transition, $H \neq 0$

In the presence of finite magnetic field H , some FM phase establishment with nonzero magnetization S_z occurs. The SR phase transition boundary can be obtained from Eqs. (18) by setting $\lambda = 0$. Thus, we obtain

$$S_z = \tanh\left[\frac{\beta_c^{(1)}}{2} (\Theta k_0 S_z + H)\right], \quad (20a)$$

$$\Omega_a = \frac{\tanh\left[\frac{\beta_c^{(1)}}{2} (\Theta k_0 S_z + H)\right]}{\Theta k_0 S_z + H}, \quad (20b)$$

where $\beta_c^{(1)} = 1/T_c^{(1)}$ is the reciprocal critical temperature of the SR phase transition in the presence of the FM state.

Further analysis of Eqs. (18) and (20) is easy to perform in two limiting cases for the temperature parameter.

The low-temperature limit presumes $\beta \gg 1$. In particular, for $\beta \Gamma_0 \gg 1$, in Eqs. (18) and (20) one can suppose that

$$\tanh\left[\frac{\beta}{2} \Gamma_0\right] \approx 1 - 2e^{-\beta \Gamma_0}. \quad (21)$$

In this case, we assume that the FM state is fully ordered, i.e., $S_z \simeq 1$, and we use Eqs. (18b) and (20b) to elucidate the SR phase transition.

Remarkably, physical temperature T in (21) may be high enough for complete graph possessing large number of nodes N in the low-temperature limit implying $T \ll \Theta N$.

Critical temperature $T_c^{(1)}$ may be obtained from (20b) by using (21) (see also Appendix); it is

$$T_c^{(1)} = \frac{\Gamma_{0,c}}{\ln\left[\frac{2}{1 - \Omega_a \Gamma_{0,c}}\right]}, \quad (22)$$

where we define $\Gamma_{0,c} \equiv \Gamma_0(\lambda = 0) = \Theta k_0 + H$ at the phase transition point $\lambda = 0$.

The SR phase transition occurs if $\beta > \beta_c^{(1)}$ or equivalently $T < T_c^{(1)}$.

Noteworthy, condition (19) at $\lambda = 0$ and Eq. (22) imply the fulfillment of inequality $\Omega_a(\Theta k_0 + H) \leq 1$ that establishes critical maximal degree $k_{c,\max} = (\frac{1}{\Omega_a} - H)/\Theta$. The SR phase can exist only for the networks possessing $k_0 \leq k_{c,\max}$. For example, the complete graph inspires critical number of nodes $N_c = \frac{1 - \Omega_a(H - \Theta)}{\Omega_a \Theta}$ obtained from (19) at $\lambda = 0$. Thereby, the SR state occurs for the networks with $N < N_c$ nodes.

On the other hand, from (20), and (10) at $S_z = 1$, $\lambda = 0$, we can obtain the critical value χ_c of coupling strength χ that looks like

$$\chi_c = \sqrt{\omega_a(h + 4Jk_0)}. \quad (23)$$

For a given network with some specified value of k_0 the SR phase occurs if transverse field coupling parameter χ obeys condition $\chi < \chi_c$. For vanishing J Eq. (23) reproduces a well-known result for the Dicke model of superradiance: the critical coupling parameter is $\chi_c = \sqrt{\hbar\omega_a}$, cf. Refs. [30–32]. Importantly, in the framework of this model the SR state dis-

appears for zero external field $h = 0$ that supports a disordered state with $S_z = 0$.

Let us establish features of the order parameter λ in the low-temperature domain. From Eqs. (18b) and (20b) accounting (21), we obtain

$$\lambda \simeq \lambda_0 \sqrt{1 - e^{(\beta_c^{(1)} - \beta)\Gamma_{0,c}}}, \quad (24)$$

where λ_0 is the order parameter at temperature $T = 0$ ($\beta \rightarrow \infty$)—see (A5) in Appendix.

In the vicinity of the critical temperature ($\beta \rightarrow \beta_c^{(1)}$) the behavior of the order parameter λ is reminiscent of familiar temperature dependence $\lambda \propto \sqrt{1 - T/T_c^{(1)}}$, which is relevant to SR second-order phase transition, cf. Ref. [34].

In the high-temperature limit, $\beta \ll 1$, we can suppose $\tanh(\frac{\beta\Gamma_0}{2}) \approx \frac{\beta\Gamma_0}{2}$ in Eqs. (18). Collective spin S_z in this limit approaches

$$S_z = \frac{\beta H}{2 - \Theta k_0 \beta}. \quad (25)$$

Equation (25) indicates the reduction of magnetization in z direction with temperature T increasing ($\beta \rightarrow 0$) or classical field H suppression.

B. Phase transitions in the limit of vanishing classical field, $H \rightarrow 0$

Here we perform analysis of Eqs. (18) in the PM-FM phase transition domain that accounts for vanishing S_z . To elucidate the phase transition features it is necessary to examine the case of vanishing classical field, $H \rightarrow 0$, in more detail. From (18) we obtain:

$$S_z = \frac{\Theta k_0 S_z}{\sqrt{(\Theta k_0 S_z)^2 + 4\lambda^2}} \tanh\left[\frac{\beta}{2} \sqrt{(\Theta k_0 S_z)^2 + 4\lambda^2}\right], \quad (26a)$$

$$\Omega_a = \frac{\tanh\left[\frac{\beta}{2} \sqrt{(\Theta k_0 S_z)^2 + 4\lambda^2}\right]}{\sqrt{(\Theta k_0 S_z)^2 + 4\lambda^2}}. \quad (26b)$$

The Eqs. (26) possess the common solution if the condition

$$\varepsilon \equiv \Theta k_0 \Omega_a = 1 \quad (27)$$

is fulfilled, cf. (19). Equations (26a) and (26b) with condition (27) are reduced to one equation,

$$\frac{1}{\Lambda} \tanh\left[\frac{\beta}{2} \Lambda\right] = \frac{1}{\Theta k_0}, \quad (28)$$

where $\Lambda \equiv \sqrt{(\Theta k_0 S_z)^2 + 4\lambda^2}$.

Noteworthy, Eq. (28) is completely symmetric in respect of collective spin S_z and photonic field amplitude λ . Thereby, we can fix one of the order parameters (say, λ) and examine the phase transition properties for another one (S_z) by solving (28).

The normal (non-SR) PM state with $S_z = 0$, $\lambda = 0$ characterizes some disordered phase for (28) formed on condition $\Lambda = 0$. Concerning nontrivial solutions of Eq. (28) we are interested in the transition from $\Lambda = 0$ to some spin ordering state with $\Lambda \neq 0$ accompanied by the SR and/or PM-FM second-order phase transitions, which are inherent to the Dicke and Ising models separately.

To be more specific, let us examine a phase boundary equation that describes the PM-FM phase transition occurring in the presence of the SR state ($\lambda = \lambda_c$). This equation can be easily obtained from (26a) for vanishing but finite $S_z \rightarrow 0$ and looks like

$$\frac{2\lambda_c}{\Theta k_0} = \tanh[\lambda_c/T_{c\lambda}^{(2)}]. \quad (29)$$

From (29) for critical temperature $T_{c\lambda}^{(2)}$ we immediately obtain

$$T_{c\lambda}^{(2)} = \frac{\lambda_c}{\tanh^{-1}\left[\frac{2\lambda_c}{\Theta k_0}\right]}. \quad (30)$$

Critical temperature $T_{c\lambda}^{(2)}$ depends on network degree k_0 , parameter Θ , and another order parameter λ_c . In particular, it follows from (29) that for $\lambda_c > \Theta k_0/2$ no phase transition occurs in the network system at any temperature. For $T < T_{c\lambda}^{(2)}$ and $\lambda < \lambda_c$ the FM SR phase represents a stable solution for the regular network system.

On the other hand, from (28) we can recognize critical temperature $T_{c,S}^{(2)}$ of the SR phase transition

$$T_{c,S}^{(2)} = \frac{\Theta k_0 S_{z,c}}{2 \tanh^{-1}[S_{z,c}]}, \quad (31)$$

setting in (28) $\lambda \simeq 0$ for $S_z = S_{z,c}$.

In the vicinity of the PM non-SR state, assuming in (29)–(31) $\lambda_c \rightarrow 0$ and $S_{z,c} \rightarrow 0$, respectively, we can use in (28) approximated formula $\tanh[\frac{\beta}{2}\Lambda] \approx \frac{\beta}{2}\Lambda$. In this limit critical temperatures (30) and (31) are equal to each other $T_{c\lambda}^{(2)} = T_{c,S}^{(2)} = T_c^{(2)}$ and tend to

$$T_c^{(2)} = \frac{1}{2} \Theta k_{0,c}. \quad (32)$$

Here, we consider the situation when the critical temperature in (32) implies the existence of critical degree $k_{0,c}$. The phase transition occurs in the networks possessing degree $k_0 < k_{0,c}$.

Remarkably, the critical temperature in (32) tends to infinity in the thermodynamic limit at $N \rightarrow \infty$ for the complete regular graph with $k_0 = N - 1$. However, in practice $T_c^{(2)}$ may be high enough but finite due to finite-size effects which determined by number of nodes N .

Figure 3 demonstrates a numerical solution of Eq. (28) established in 3D space by using S_z and λ variables. We examine here the particular case $\Theta k_0 = \Omega_a = 1$ for (27) and (28). The SR FM domain appears within temperature window $0 \leq T < T_c^{(2)}$ as a result of intersection of σ plane ($z = \frac{1}{\Theta k_0} = 1$) with a surface representing function $F(S_z, \lambda) = \frac{1}{\Lambda} \tanh[\frac{\beta}{2}\Lambda]$, which is relevant to the left side of (28). Clearly, the size of the domain is maximal in the zero-temperature limit, see the black solid curve AB in Fig. 3. This domain is characterized by equation $\sqrt{(\Theta k_0 S_z)^2 + 4\lambda^2} = \Theta k_0$ that may be obtained from (28). Obviously, the domain reduces with the temperature increasing up to $T_c^{(2)} = 1/2$, see the red curves in Fig. 3.

The results obtained in Eqs. (30)–(32) admit a simple physical interpretation given in Fig. 3.

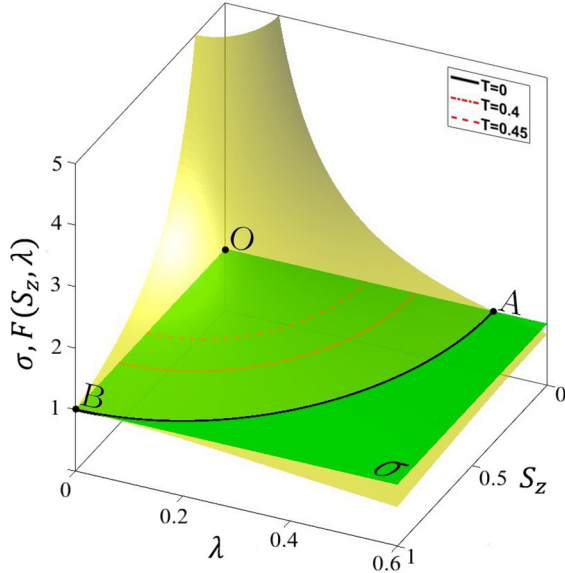


FIG. 3. Function $F(S_z, \lambda)$ (yellow surface), σ plane (green plane) vs. S_z and λ for $\Theta k_0 = \Omega_a = 1$ and temperature $T = 0$. The point O indicates the PM normal (non-SR) state. The lines OA and OB correspond to the SR PM and normal FM phases, respectively, which occur within the suitable temperature domain. The red curves indicate the solutions of (28) at two different temperatures [$F(S_z, \lambda)$ is not shown for them].

The point O in Fig. 3 with coordinates $S_z = \lambda = 0$ characterizes the disordered (PM non-SR) state $\Lambda = 0$ being a solution of Eq. (28) at temperature $T_c^{(2)}$, cf. (32).

The line OB represents the phase boundary for the SR phase transition in the presence of some FM state relevant to nonzero $S_{z,c}$ and characterized by critical temperature $T_{c,S}^{(2)}$ defined in (31).

Remarkably, the line OA represents the PM-FM phase boundary in the presence of superradiance. Various values of λ_c on OA are inherent to critical temperature $T_{c,\lambda}^{(2)}$. For example, the point A corresponds to the phase transition at zero critical temperature that implies $\lambda_c = \Theta k_0/2$, cf. (29). By means of definition (4), for $N \gg 1$, we can represent critical photon number $N_{\text{ph},c}$ required to achieve the phase transition for the complete graph as

$$N_{\text{ph},c} \simeq \frac{\Theta^2 N^3}{4}. \quad (33)$$

In some applications of the SR phase transition in photonics two limiting cases are usually considered. First, we can speak about convenient lasing phenomena when the number of photons is much larger than the number of particles (nodes in our case), cf. Refs. [34,36]. Another limit that implies fulfillment of inequality $N_{\text{ph}} \ll N$ is typically considered in the framework of polariton lasers occurring in the strong matter-field coupling regime [36,42,43]. These limits appear in experiments with exciton polariton BEC as two thresholds to the lasing effects, which possess different physical background [43,56]. For the network system inequality $N_{\text{ph},c} \ll N$ applied to the critical photon number $N_{\text{ph},c}$ together with (33) implies that dimensionless spin-spin interaction strength Θ

obeys the condition $\Theta \ll 2/N$. Since number of nodes N is huge for many practical applications [22,23], Θ should be small enough in this limit.

V. PHASE TRANSITIONS IN COMPLEX NETWORKS

A. Superradiant phase transition in the random and scale-free networks

1. Phase transitions in $H \rightarrow 0$ limit

Now let us consider the phase transitions in the random and scale-free networks by means of Eqs. (11). Unfortunately, due to large set of parameters occurring in the Dicke-Ising model, it is hard to examine (11) analytically in a general case. Here we represent some important limiting cases, which admit simple treatments for the critical parameters obtained under the phase transition condition. In particular, (11) for $H = 0$ yields

$$F_1(S_z, \lambda) \equiv \int_{k_{\min}}^{k_{\max}} p(k) \frac{\Theta k^2}{\Gamma \langle k \rangle} \tanh \left[\frac{\beta}{2} \Gamma \right] dk = 1, \quad (34a)$$

$$F_2(S_z, \lambda) \equiv \frac{1}{\Omega_a} \int_{k_{\min}}^{k_{\max}} p(k) \frac{\tanh \left[\frac{\beta}{2} \Gamma \right]}{\Gamma} dk = 1, \quad (34b)$$

where $\Gamma \equiv \sqrt{(\Theta S_z k)^2 + 4\lambda^2}$.

In a general case, critical temperature T_c of the SR phase transition for the complex networks essentially depends on particular degree distribution $p(k)$. The physical explanation of this fact looks as following.

The random and especially scale-free networks considered here support a locally (node) dependent interaction between the spins because of some specific topological features (hubs, clusters, etc.). This interaction leads to the existence of effective local field [see Eq. (5)] responsible for the establishment of some FM ordering in the z direction even without external magnetic field H . Thus, the SR phase transition appears as a result of the interplay between spin ordering in z and x directions and depends on topological features of the network in $\lambda \rightarrow 0$ limit.

In Fig. 4 we examine solutions of Eqs. (34) numerically. In particular, Fig. 4(a) displays the solution of Eqs. (34) for the BA network. We take the parameters $\Omega_a = 1$, $\Theta \langle k \rangle = 1$, which are maximally close to the ones for Fig. 3. Graphically, this solution looks as the crossing point C for σ plane and functionals $F_1(S_z, \lambda)$ (yellow surface) and $F_2(S_z, \lambda)$ (blue surface), which represent the left-hand sides of Eqs. (34a) and (34b), respectively, cf. Fig. 3. The intersection lines AD and BE confine the domains of the FM and/or SR phases, which correspond to the solutions of Eqs. (34a) and (34b) separately. The dashed red line restricts the area where the FM and SR phases coexist. This area is maximal at zero temperature.

Thus, the only one crossing point C in Fig. 4(a) separates different phases, while in Fig. 3 this role is performed by the curve, which implies the phase boundaries in the OA and OB directions.

Figure 4(b) establishes the numerical solutions of Eqs. (34) for various temperatures and values of γ for the scale-free (crosses, triangles) and random (circles) networks. The solution of Eqs. (34) for scale-free networks exists within the domain $2 < \gamma \leq 3.75$, where $\langle k \rangle$ possesses moderate val-

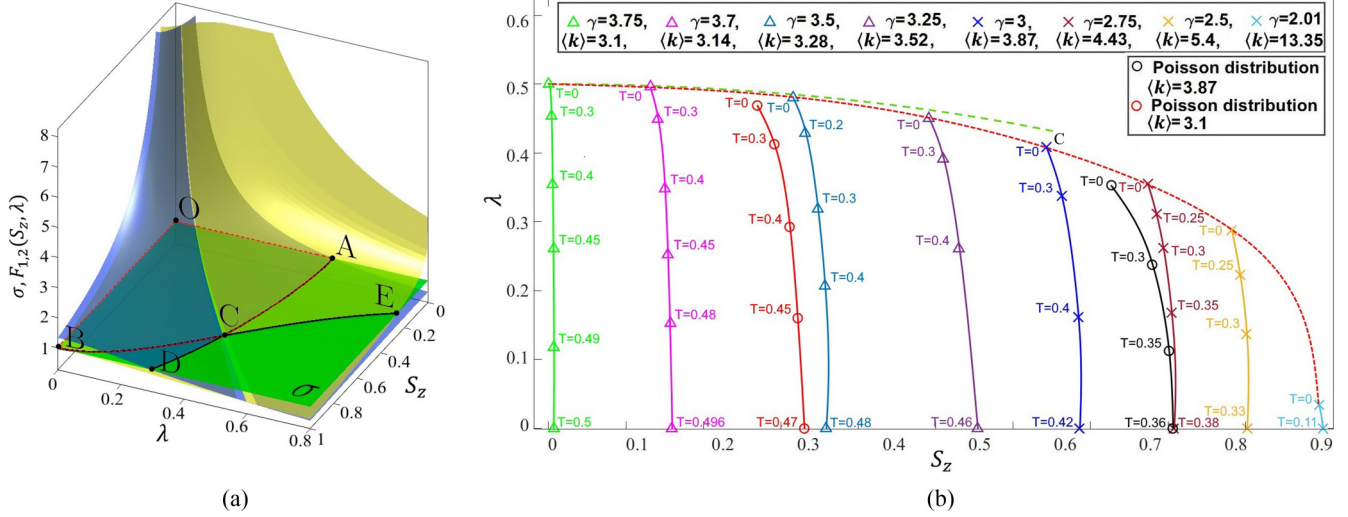


FIG. 4. (a) Functionals F_1 (yellow surface), F_2 (blue surface), and σ plane (green plane) vs. S_z and λ at temperature $T = 0$ and for $\gamma = 3$. (b) Phase boundaries for the crossing points in the λ - S_z plane. The parameters are as follows: $\Theta = 0.25$, $\Omega_a = 1$, and $N = 1000$. The maximal (minimal) degree for the scale-free networks are $k_{\max} = k_{\min} N^{\frac{1}{\gamma-1}}$ ($k_{\min} = 2$). For the random networks $k_{\max} = 11$ (for $\langle k \rangle = 3.87$) and $k_{\max} = 9$ (for $\langle k \rangle = 3.1$) with $k_{\min} = 0$ are used, respectively. The green dashed line represent solution of Eqs. (35). See more details in the text.

ues, see Fig. 2. For example, consider the dark blue curve in Fig. 4(b) (marked by crosses) that corresponds to the BA network with $\gamma = 3$. The curve starts at $T = 0$ in the crossing point C, which is the same point as in Fig. 4(a), and then moves toward S_z axis with the temperature increasing. Critical temperature T_c of the phase transition to the superradiance is obtained at the point where $\lambda = 0$; it is equal to $T_c = 0.42$. The functional in (34a) for this point is $F_1(S_z, 0) = \int_{k_{\min}}^{k_{\max}} p(k) \frac{k}{S_z} \tanh[\frac{\beta_c}{2} \Theta k S_z] dk$ and corresponds to the FM state with $S_z \simeq 0.68$, see Fig. 4(b). This feature of $F_1(S_z, 0)$ manifests the SR phase transition in the presence of the FM state that occurs at zero external field H , cf. Fig. 3.

The dashed red line in Fig. 4(b) indicates the fact that T_c diminishes for the scale-free network with γ reduction. Simultaneously, the value of magnetization S_z increases. This is not surprising, since without the external classical field, $H = 0$, the network spin system aspires to increase the ordering state at lower temperatures. In particular, Eqs. (34) admit of the point in the λ - S_z plane [marked by bright blue crosses in Fig. 4(b)] that corresponds to the ordered collective spin state ($S_z \simeq 1$) obtained at critical temperature $T_c \simeq 0.11$ for $\gamma = 2.01$.

Remarkably, the same dashed (red) curve in Fig. 4(b) exhibits vanishing of the order parameter λ with increasing average degree $\langle k \rangle$. We can elucidate this feature of the Dicke-Ising model examining the asymptotic solution of (34) in zero-temperature limit. We assume in (34) that $\Gamma \simeq \bar{\Gamma} \equiv \sqrt{(\Theta S_z \langle k \rangle)^2 + 4\lambda^2}$, supposing that approach $k \simeq \langle k \rangle$ is valid. In this limiting case from (34) we obtain

$$\Omega_a \Theta \zeta = 1, \quad (35a)$$

$$\Omega_a \bar{\Gamma} = 1. \quad (35b)$$

The green dashed curve in Fig. 4(b) represents the solution of Eqs. (35) for $\langle k \rangle = 3.1$ ($\zeta \simeq 4$). From Fig. 4(b) it is clearly seen that the approach we use here is valid within degree exponent $3.75 \leq \gamma \leq 3.25$, where the green dashed

line approaches the red one, which is relevant to numerical solutions of (34). For $\gamma < 3.25$ the discrepancy between two dashed curves of Eq. (35) do not exist.

The phase boundaries for the random networks are represented in Fig. 4(b) by two (red and black coloured) curves with circles. To find the upper natural cutoff k_{\max} we explore arguments represented in Sec. III. The difference between the curves is determined by the value of $\langle k \rangle$ and exhibits general tendency of vanishing λ with increasing $\langle k \rangle$.

Now let us analytically examine Eqs. (34) when they admit some simplifications. Remarkably, Eqs. (34) possess simple treatments for the PM-FM phase transition boundary that occurs in the complex networks at some SR state, for given λ_c and vanishing S_z . In particular, the green curve with triangles in Fig. 4(b) is relevant to this limit. Solving Eqs. (34) in the limit of vanishing S_z for the critical temperature we get

$$T_c = \frac{\lambda_c}{\tanh^{-1} \left[\frac{2\lambda_c}{\Theta \zeta} \right]} \quad (36)$$

with condition (35a) that accounts for the solution of (34b) in the same limit, cf. (27).

Equation (36) represents a generalization of (30) obtained for the regular networks. The topological properties of the network in (36) are taken into account at the macroscopic level using the ζ parameter.

In the vicinity of the disordered state at $S_z \sim 0$, $\lambda \sim 0$ Eq. (34) simplifies; for the critical temperature of the transition to the ordered state we can obtain

$$T_c = \frac{1}{2} \Theta \zeta. \quad (37)$$

Equation (37) represents a generalization of Eq. (32) for the complex networks in the Dicke-Ising model framework; in (37) and thereafter we omit the upper indices for the critical temperature. It is noteworthy that the critical temperature (37) obtained for Dicke-Ising model coincides with that for the

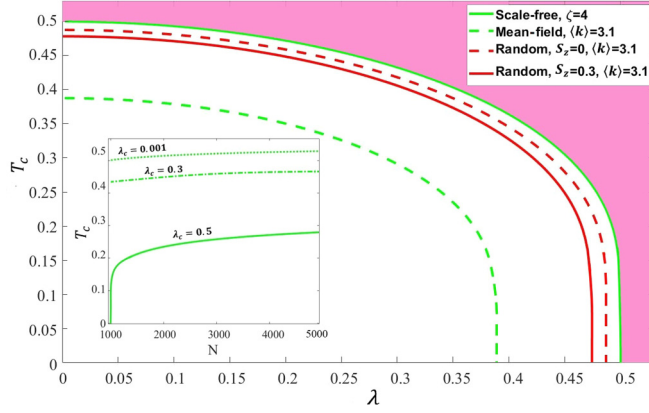


FIG. 5. Dependence of temperature T versus order parameter λ for the scale-free network (green curves) with $\gamma = 3.75$, $S_z \simeq 0$ and random one with $S_z \simeq 0.3$ (solid red curve), $S_z \simeq 0$ (dashed red curve), respectively. The parameters are as follows: $\Theta = 0.25$, $\Omega_a = 1$, $N = 1000$, and $\langle k \rangle = 3.1$, cf. Fig. 4(b). The shadow region corresponds to the PM phase $S_z = 0$. The inset indicates the dependence of critical temperature T_c on number of nodes N calculated for the same scale-free network at different λ_c .

Ising model on networks, cf. Refs. [14,19,22,24]. Moreover, this critical temperature agrees with results obtained rigorously by other approaches, cf. Refs. [1,18].

From (36) and (37) it follows that since $\zeta \rightarrow \infty$ for the scale-free network in the thermodynamic limit, the critical temperature of the PM-FM phase transition is also infinite. However, the finite critical temperature for the phase transition occurs in (37) due to the finite-size effects for the scale-free network, see Table I.

In Fig. 5 we plot dependence (36) for the critical temperature T_c of PM-FM phase transition versus order parameter λ for the scale-free (green curves) and random (the red dashed curve) networks, respectively. The parameters for the scale-free network in Fig. 4 are relevant to the ones established for the green curve with triangles in Fig. 4(b). The phase boundaries shown in Fig. 5 separate the PM state (it is shown as a shadow region for the scale-free network) and the FM SR state. Notably, (37) may be obtained from (36) in the limit of $\lambda_c \rightarrow 0$. In particular, the crossing point of the solid green curve in Fig. 5 with line $\lambda = 0$ determines the critical temperature established by Eq. (37) for the scale-free network. In this limit PM-FM phase transition leads to establishment of some ordering FM non-SR state.

It is instructive to compare Eqs. (36) and (37) with the results obtained in the framework of other mean-field theories suitable for the Ising model, see Refs. [14,19,26]. In Ref. [26] authors consider the approximation of the Ising model on a BA network by the effective long-range homogeneous Ising model providing effective spin-spin interaction strength determined through the average degree of the BA network. The result for the effective long-range Ising model may be obtained from (37) setting $\zeta \simeq \langle k \rangle$ that implies $\langle k^2 \rangle \approx \langle k \rangle^2$. Physically, such a condition means “homogenization” of the scale-free network, which may be relevant for large degree exponent γ , cf. Ref. [14]. As it follows from Table I, such an approximation error for the effective long-range Ising model

grows with the number of nodes N as $\zeta / \langle k \rangle = \frac{1}{4} \ln(N)$. Moreover, as it follows from Fig. 2, discrepancy between ζ and $\langle k \rangle$ is large enough within domain $1 < \gamma < 3$, where the effective long-range Ising model seems to be inapplicable.

To be more specific, in Fig. 5 we examine the effective long-range Ising model for the scale-free network with degree exponent $\gamma = 3.75$; the dashed green curve in Fig. 5 represents the phase boundary in this case. This mean-field approach accuracy may be estimated from Table I; it is determined by ratio $\zeta / \langle k \rangle \simeq 1.5(1 - N^{-3/11}) \approx 1.26$ with $N = 1000$. In this approximation the critical temperature (36) for the scale-free network behaves as $T_c = \lambda_c / \tanh^{-1}[\frac{2\lambda_c}{\Theta \langle k \rangle}]$, which is reminiscent to the regular network with $\langle k \rangle = k_0$, cf. (30) and Ref. [26]. Thereby, some discrepancies for the green curves in Fig. 5 may be explained due to the scale-free network “homogenization” procedure.

Red curves in Fig. 5 establish temperature dependence for random networks. The dashed curve represents phase boundary in accordance with Eq. (36), i.e., in the limit of $S_z = 0$. However, as it follows from numerical simulations given in Fig. 4(b) we can treat collective spin S_z in (34) as some constant possessing average value within temperature domain being under consideration if the variation of S_z with temperature is not so large.

In Fig. 5 we represent the solid red curve for the random network possessing $S_z \approx 0.3$ and relevant to the red curve with circles in Fig. 4(b). Within this limit the temperature dependence on λ is obtained from (34a) and approaches

$$T = \frac{\bar{\Gamma}}{2 \tanh^{-1}[\frac{\bar{\Gamma}}{\Theta \zeta}]}. \quad (38)$$

As clearly seen from Fig. 5, for moderate values of collective spin S_z and coupling strength Θ the temperature dependence (the dashed curve) approaches its phase boundary. At the same time, dependence for the random networks is close to the solid green curve that characterizes the scale-free network in the random domain, cf. Ref. [3].

The finite-size effects may be obtained from the last column in Table I that displays the critical number of nodes, which is required to obtain phase transition for a given network system. As example, from (36) for the BA scale-free network that imposes $\gamma = 3$ the critical temperature of the phase transition is $T_c = \frac{1}{8} \Theta \langle k \rangle \ln(N_c)$ that immediately defines the critical number of nodes

$$N_c = e^{8T_c / \Theta \langle k \rangle}. \quad (39)$$

Equation (39) implies critical clustering coefficient $\langle C_c \rangle \sim [\ln(N_c)]^2 / N_c$ permissible for the phase transition.

The inset in Fig. 5 exhibits the behavior of critical temperature T_c on number of nodes N as it follows from (36). Since the number of nodes N is large enough, we restrict ourselves to region $N \geq 1000$. The curves in Fig. 5 inset constrain the region of superradiance. In particular, these curves demonstrate that critical temperature T_c grows starting from some certain value that corresponds to the critical number of nodes where the solution of (36) exists.

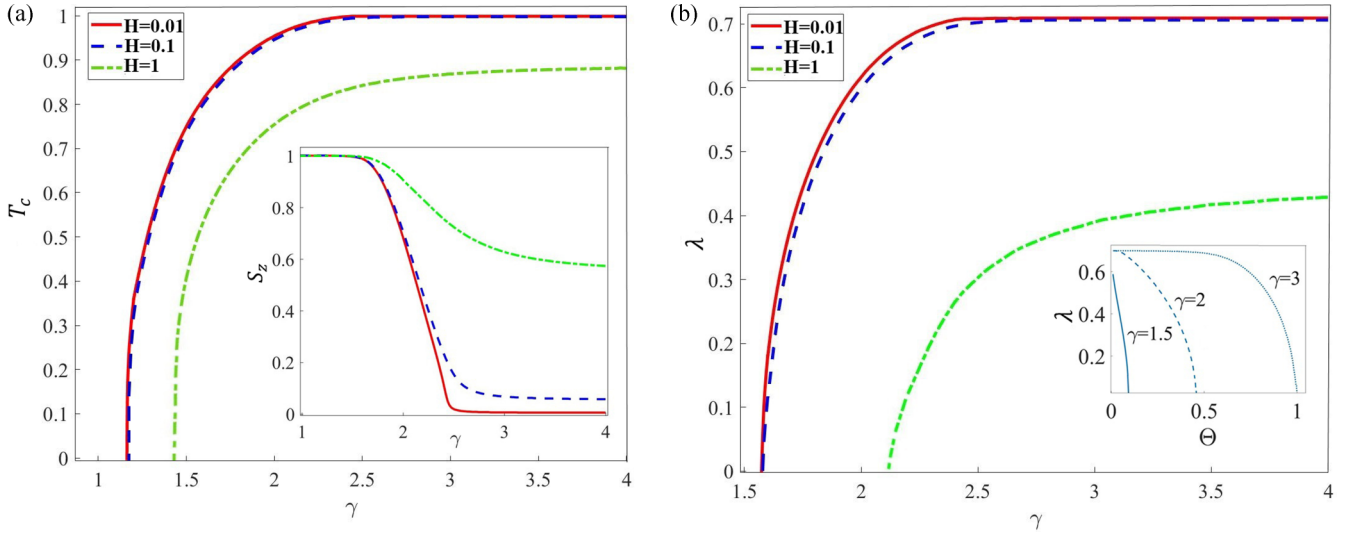


FIG. 6. Dependence of (a) critical temperature T_c and (b) order parameter λ vs. γ . The parameters are as follows: $\Theta = 0.15$, $N = 1000$, $\Omega_a = 0.5$, $k_{\min} = 1$, $k_{\max} = k_{\min} N^{\frac{1}{\gamma-1}}$ for (a) $-\lambda = 0$, and for (b) $T = 0.8$, respectively; $\langle k \rangle$ specified in Table I. The inset in (a) exhibits total spin component S_z vs. γ for the dependence given in (b) at $T = 0.8$. The inset in (b) demonstrates the dependence of λ on Θ at $H = 0.1$ and $T = 0.8$ but for different values of γ : $\gamma = 1.5$, $\gamma = 2$, and $\gamma = 3$.

2. Phase transitions at nonvanishing classical field H and for scale-free networks

The aim of this part is to study the phase transition problem for the scale-free network within a large domain of power degree γ and nonvanishing classical field H . We now search for nontrivial solutions $\lambda \neq 0$ and $S_z \neq 0$ of Eqs. (11).

In Fig. 6 we represent numerical solutions of Eqs. (11) for critical temperature T_c and order parameter λ as functions of γ .

Notice, collective spin component S_z , as it follows from Fig. 6(a), approaches the FM state within the domain $1 < \gamma < 1.7$ of the anomalous regime for the scale-free networks. Roughly speaking, the spin system exhibits the fully ordered state. Figure 6(b) shows that the influence of another order parameter λ is not so important in the anomalous regime where $S_z \simeq 1$. In fact, in this case we deal with the situation valid for the familiar Ising model without the transverse field. Moreover, the thermal fluctuations have no ability to break the FM state at any finite temperatures within the domain $1 < \gamma < 3$, cf. Ref. [1].

The behavior of the spin system within $1 < \gamma < 1.7$ domain completely depends on average degree $\langle k \rangle$ that grows rapidly, as it follows from Fig. 2. In particular, in the anomalous regime the size of the largest hub $k_{\max} \propto N^{\frac{1}{\gamma-1}} > N$, and the number of links connected to the largest hub increases faster than the size of the network, N . We expect to obtain a strong spin-spin interaction within this domain. Thus, we assume that randomly chosen k possesses large values due to the power-law degree $p(k)$, see Fig. 1(d). In this case, for large k we can use approximation $\tanh[\frac{\beta}{2}(\Theta S_z k + H)] \approx 1$ in Eq. (11a), which allows to obtain $S_z \simeq 1$ for the collective spin, see the inset in Fig. 6(a).

Remarkably, in the anomalous regime the main contribution to effective magnetic field H_{eff} comes from the term that characterizes the spin-spin interaction and depends on

network parameter $\langle k \rangle$, see (5) and (6). From Fig. 6 we can see that behavior of the spin system for small values of external field H (the red and blue curves) are practically still the same.

In the presence of the interaction with the quantized transverse field, S_z abruptly vanishes at small values of classical magnetic field H , which is clearly seen from the inset in Fig. 6(a). In Fig. 4(b), we have already specified this behavior of S_z within the scale-free and random domains ($2 < \gamma \leq 3.75$), respectively.

In particular, we perform the analysis of Eqs. (11) in the relatively high-temperature limit for nonzero field H ; the spontaneous magnetization can be represented in the following form [cf. (25)]

$$S_z = \frac{\beta H}{2 - \beta \Theta \zeta}, \quad (40)$$

that defines the FM state with vanishing S_z in the presence of superradiance. S_z approaches some constant value $S_z \approx \frac{\beta H}{2}$ for vanishing ζ that clearly exhibits the dependence of S_z in the inset in Fig. 6(a) in the network system.

This happens due to the critical temperature increasing and establishing the finite superradiant field amplitude λ that characterizes the magnetization in x direction; critical temperature T_c in Fig. 6(a) approaches some nonzero value for $\gamma \geq 2.5$. In particular, the superradiant field promotes the spin flipping that occurs on the scale-free network nodes, see Fig. 6(b). In other words, the establishment of nonvanishing transverse field introduces some disordering in the collective spin component in z direction. In contrast, classical magnetic field H tends to preserve the ordered state of collective spin S_z , see the green curves in Fig. 6(a) which are plotted for value $H = 1$. The absolute value of the established superradiant field amplitude λ vanishes in this case, see the green curve in Fig. 6(b).

The inset in Fig. 6(b) demonstrates the suppression of order parameter λ with increasing of Θ . Such a behavior happens

due to the contribution of the spin-spin interaction energy into total magnetization in z direction. As it follows from Eqs. (5) and (6) the increasing of Θ for a given degree exponent γ leads to the increasing of effective field H_{eff} that enhances magnetization in z direction suppressing it in the x direction. For the degree exponent less than two, the domain where the SR state exists, $\lambda \neq 1$, is narrow enough, see the solid curve with $\gamma = 1.5$ in the inset in Fig. 6(b). As we discussed before, in this case the spin system possesses some ordered state, as it is shown in the inset in Fig. 6(a). At larger values of degree exponent γ , the SR state domain exists within a large Θ -parameter window [that the inset in Fig. 6(b) indicates] due to establishing of the nonvanishing superradiant field for $\gamma > 2$, as it is shown in Fig. 6(b).

B. Quantum phase transitions

The quantum phase transition is obtained in the zero-temperature limit setting in Eqs. (11) $\beta \rightarrow \infty$ that presumes $\tanh(\frac{\beta}{2}\Gamma) \simeq 1$. From (11) for small-enough λ in this case we obtain:

$$S_z = 1 - \frac{2\lambda^2}{\langle k \rangle} \int_{k_{\min}}^{k_{\max}} \frac{k p(k)}{(\Theta S_z k + H)^2} dk, \quad (41a)$$

$$\Omega_a = \int_{k_{\min}}^{k_{\max}} \frac{p(k)}{(\Theta S_z k + H)} \left[1 - \frac{2\lambda^2}{(\Theta S_z k + H)^2} \right] dk. \quad (41b)$$

As clearly seen from Eqs. (41), the spin system is fully ordered, i.e., $S_z = 1$ for $\lambda = 0$. This situation agrees with the results obtained for Fig. 4(b) (the bright blue curve) and Fig. 6(a) at nonzero temperatures and relatively small γ .

The SR quantum phase transition, with $S_z = 1$, occurs for the critical value of transverse field frequency $\Omega_{a,c}$ that is determined from (41b) and looks like

$$\Omega_{a,c} = \int_{k_{\min}}^{k_{\max}} \frac{p(k)}{\Theta k + H} dk. \quad (42)$$

Equations (41b) and (42) result in a simple dependence for order parameter λ

$$\lambda = \lambda_0 \sqrt{1 - \frac{\Omega_a}{\Omega_{a,c}}}, \quad (43)$$

where $\lambda_0 = \sqrt{\frac{\Omega_{a,c}}{2I}}$ is the order parameter in the limit $\Omega_a \rightarrow 0$, $I \equiv \int_{k_{\min}}^{k_{\max}} \frac{p(k)}{(\Theta S_z k + H)^3} dk$.

We can simplify Eqs. (42) and (43) in the vicinity of $H = 0$ for the FM state, $S_z = 1$. In particular, for the regular network we obtain $\lambda_0 = 0.71\Theta k_0 \equiv 0.71\Theta \langle k \rangle$, cf. Fig. 3. For the BA network possessing very large number of nodes N we get $\lambda_0 \simeq 0.46\Theta \langle k \rangle$, see Table I, $\gamma = 3$. Thereby, the approach used in Eq. (43) is valid for the network parameters obeying condition $\Theta \langle k \rangle \ll 1$.

On the other hand, for finite field H close to the disordered state with $S_z = 0$ from Eq. (43), we can deduce that the quantum phase transition has no dependency on the network characteristics and results in the establishment of small transverse, m_x , and longitudinal, m_z , magnetizations proportional to $\lambda_0 = H/\sqrt{2} \ll 1$ and $\Omega_a/\Omega_{a,c} \ll 1$, respectively.

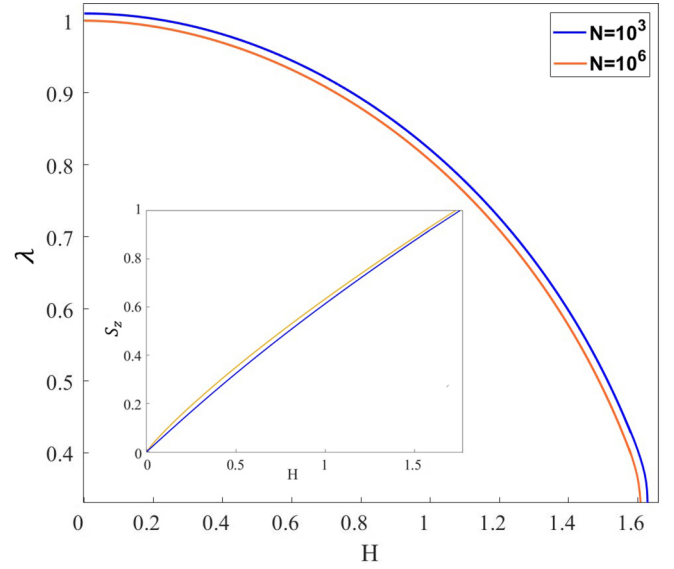


FIG. 7. Order parameter λ versus local field H for the BA network, $\gamma = 3$, at $T_c = 0$ for different number of node N . The dependence of magnetization S_z on H is shown in the inset. Other parameters are as follows: $\Omega_a = 0.5$, $\Theta = 0.15$, $k_{\min} = 1$, $k_{\max} = k_{\min}\sqrt{N}$.

In Fig. 7 we plot the dependence of the order parameters λ and S_z as functions of the magnetic field H , which represent the numerical solutions of Eqs. (11) for the BA network with different number of nodes N in the zero-temperature limit. The SR quantum phase transition occurs for nonzero H when the magnetization attained the FM state with $S_z = 1$. In the vicinity of the phase transition point H_c , the order parameter λ behaves as $\lambda \propto \sqrt{1 - H/H_c}$, cf. (43).

VI. CONCLUSION

To summarize, we have considered the problem of the superradiant phase transition in the network structures. The Dicke-Ising model is developed to elucidate the second-order phase transition for the regular, random, and scale-free networks. The model concerns the spin-1/2 (two-level) systems located in the network nodes and placed in the local classical magnetic and weak quantum transverse (photonic) fields. Applying the mean-field approach, familiar in quantum optics, we have obtained the set of Eqs. (11), which describes two order parameters S_z and λ relevant to magnetization along z and x axes, respectively. In particular, Eq. (11a) characterizes the collective weighted spin z component, S_z . It is relevant to the PM-FM phase transition problem. Equation (11b) establishes the normalized transverse field amplitude, λ , which corresponds to the phase transition to the superradiance for the spin network system. The SR state with $\lambda \neq 0$ is characterized by a non-zero-temperature dependent energy gap that takes place for the spin system.

To be more specific, we have examined the annealed networks with the regular (fixed) degree number, the random network with the Poisson degree distribution, and the scale-free networks possessing the power-law degree distri-

bution with degree exponent γ that inherent to the region $1 < \gamma \leq 4$.

We have considered the problem of the phase transition for the Dicke-Ising model in two limits of classical field H . The superradiance occurs in the ferromagnetic spin system in the limit of the finite (nonzero) classical magnetic field. For the regular networks we have obtained analytically a simple equation (24) analogous to the familiar law of temperature dependence for the gap systems (superconductors, ensemble of two-level systems interacting with quantized electromagnetic field) possessing the continuous second-order phase transition. In this case, the transition to the SR state is followed by the establishment of the spontaneous magnetization with the quantum transverse field in x direction. For the network that represents a complete graph, the critical number of nodes defines the necessary condition to attain the SR state.

The physical picture becomes richer and more complicated for vanishing classical external field H . We have shown that for the regular networks Eqs. (11) reduce to one (gaplike) equation (28), which is completely symmetric in respect of order parameters S_z and λ . Physically, we can recognize the phase transition occurring in the network system at the critical temperature as a crossover from the disordered state with $S_z = 0$, $\lambda = 0$ to some ordered state possessing $S_z \neq 0$ (FM state) and/or $\lambda = 0$ (SR state).

To achieve the ordering state for the regular networks possessing constant degree k_0 , one can fix vanishing collective spin S_z and then consider the SR phase transition across order parameter λ . Alternatively, we can fix λ and then obtain the PM-FM phase transition.

It is important to note that in the $S_z \simeq 0$ and $\lambda \simeq 0$ limits the critical temperature of the disorder-order phase transition for examined networks exhibit the finite-size effects. Remarkably, our mean-field approach allows to account degree correlations in the scale-free network structure which we describe by the parameter ζ , see (13). In particular, the obtained critical temperature may be high enough but finite; it depends on average degree $\langle k \rangle$ for the regular network and statistical properties (ζ parameter) for the scale-free and random networks, respectively. The analytical and numerical simulations which we performed for the scale-free networks within scale-free and random regimes, allow to conclude that the order parameter, λ , vanishes with increasing average degree $\langle k \rangle$ and increasing collective spin component S_z . The ‘‘homogenization’’ of the scale-free network structure, that presumes $\zeta \approx \langle k \rangle$, may be relevant for large degree exponent γ . In this sense, our results agree with the ones obtained for the scale-free networks possessing the power degree distribution achieved by other methods, cf. Refs. [14,19]. As seen from Fig. 5 (the green curves), the mean-field approach based on scale-free network ‘‘homogenization’’ leads to some discrepancies within critical temperature region, cf. Ref. [26].

In general, the features of the complex networks phase transition strictly depend on power degree γ . In the anomalous regime, $1 < \gamma < 2$, the effective spin-spin interaction, which may be described in terms of effective magnetic field, see (5) and (6), dominates due to large average degree $\langle k \rangle$. In particular, at low γ the FM state with $S_z = 1$ establishes; this state is very hard to alter by means of the spin interaction with the weak quantized field or even with the moderate

external magnetic field. However, the situation changes with γ increasing. Diminishing the effective spin-spin interaction leads to the suppression of collective S_z spin component and creates an enabling environment for the PM-FM and SR phase transitions, see Fig. 4 and Fig. 6, respectively. In the scale-free domain, $2 < \gamma < 3$, the ordering in the network spin system appears as a result of the interplay between magnetizations in x and z directions. The SR phase transition in this domain occurs for some FM state, see Fig. 4(b).

Finally, we have examined the quantum phase transition that happens in the zero-temperature limit. We have demonstrated that the transverse field amplitude λ exhibits a familiar scaling as a function of frequency Ω_a . For vanishing H the maximal value of the field is characterized by degree $\langle k \rangle$ and spin-spin interaction energy J . In fact, this phase transition disappears for the Dicke model with $J = 0$.

It is remarkable that the results obtained can be useful for studying the controllability problem in the complex networks which may represent distributed (natural, or artificial) intelligence systems (DIS) cf. [53,57]. In particular, the Dicke-Ising model that we analyse in this work is relevant to the modeling of finite temperature (i.e. finite network size) phase transitions occurring in scale-free network DIS's which we model by means of interacting two-level systems and which we represented as a simple quantum-like agents of decision making. The quantized (transverse) field represents an additional degree of freedom for this problem. In a more general case it is necessary to examine the limit when each node interacts with its own (local) quantized transverse field.

ACKNOWLEDGMENTS

This work was financially supported by the Ministry of Science and Higher Education of Russian Federation, Goszadanie No. 2019-1339.

APPENDIX: PHASE TRANSITIONS AT LOW- AND HIGH-TEMPERATURE LIMITS

Let us briefly discuss the main properties of the regular networks at low temperatures $\beta \gg 1$. Eq. (18b) in the limit of (21) may be rewritten as (cf. Ref. [55])

$$\Omega_a \Gamma_0 = 1 - 2e^{-\beta \Gamma_0}, \quad (\text{A1})$$

where $\Gamma_0 = \sqrt{(\Theta k_0 + H)^2 + 4\lambda^2}$. We assume that at low-enough temperatures the spin system possesses the FM state with $S_z \simeq 1$.

At critical temperature $T_c^{(1)} \equiv 1/\beta_c^{(1)}$ Eq. (A1) looks like

$$\Omega_a \Gamma_{0,c} = 1 - 2e^{-\beta_c^{(1)} \Gamma_{0,c}}, \quad (\text{A2})$$

where we define $\Gamma_{0,c} \equiv \Gamma_0(\lambda = 0) = \Theta k_0 + H$ at the phase transition point $\lambda = 0$. Inverting (A2) for the critical temperature of phase transition $T_c^{(1)}$ one can immediately obtain (22).

On the other hand, at zero temperature Eq. (A1) implies

$$\Omega_a \Gamma_{0,0} = 1, \quad (\text{A3})$$

where we denote $\Gamma_{0,0} \equiv \sqrt{\Gamma_{0,c}^2 + 4\lambda_0^2}$ and introduce λ_0 as a maximal value of the order parameter obtained at $T = 0$.

To find λ_0 we assume that it is sufficiently small in the low-temperature domain (cf. Ref. [42]), i.e., we suppose that $\lambda_0^2 \ll 1$, and for $\Gamma_{0,0}$ we can use approximation

$$\Gamma_{0,0} \approx \Gamma_{0,c} \left(1 + \frac{2\lambda_0^2}{\Gamma_{0,c}^2} \right). \quad (\text{A4})$$

Substituting (A4) into (A3) and combining it with (A2) after some straightforward calculations we obtain

$$\lambda_0 = \Gamma_{0,c} e^{-\frac{1}{2}\beta_c^{(1)}\Gamma_{0,c}}. \quad (\text{A5})$$

Then we can find the temperature dependence for order parameter λ from Eqs. (A1) and (A2) leading to

$$\frac{\Gamma_0}{\Gamma_{0,c}} \simeq \frac{1 - 2e^{-\beta\Gamma_{0,c}}}{1 - 2e^{-\beta_c^{(1)}\Gamma_{0,c}}}. \quad (\text{A6})$$

In (A6) we use (A4) and also assume that condition $\beta\lambda^2/\Gamma_{0,c} \ll 1$ is fulfilled within the low-temperature limit domain.

Finally, after some calculations from (A6) we obtain (24) by means of (A4) and (A5).

-
- [1] S. Dorogovtsev, *Lectures on Complex Networks*, Oxford Master Series in Physics, Vol. 20 (Oxford University Press, Oxford, 2010).
- [2] M. Newman, *Networks* (Oxford University Press, Oxford, 2018), p. 727.
- [3] Albert-László Barabási, *Network Science* (Cambridge University Press, Cambridge, 2016), p. 475.
- [4] S. Fortunato and D. Hric, Community detection in networks: A user guide, *Phys. Rep.* **659**, 1 (2016).
- [5] D. Easley and J. Kleinberg, *Networks, Crowds, and Markets* (Cambridge University Press, Cambridge, 2010), p. 727.
- [6] J. Krishnan, R. Torabi, A. Schuppert, and E. Di Napoli, A modified Ising model of Barabási-Albert network with gene-type spins, *J. Math. Biol.* **81**, 769 (2020).
- [7] S. E. Ahnert, W. P. Grant, and C. J. Pickard, Revealing and exploiting hierarchical material structure through complex atomic networks, *npj Comput. Mater.* **3**, 35 (2017).
- [8] G. Bianconi, Superconductor-insulator transition on annealed complex networks, *Phys. Rev. E* **85**, 061113 (2012).
- [9] Z.-L. Xiang, S. Ashhab, J. Q. You, and F. Nori, Hybrid quantum circuits: Superconducting circuits interacting with other quantum systems, *Rev. Mod. Phys.* **85**, 623 (2013).
- [10] A. Barrat, M. Barthélemy, and A. Vespignani, *Dynamical Processes on Complex Networks* (Cambridge University Press, Cambridge, 2008), p. 366.
- [11] S. Brito, A. Canabarro, R. Chaves, and D. Cavalcanti, Statistical Properties of the Quantum Internet, *Phys. Rev. Lett.* **124**, 210501 (2020).
- [12] E. Bullmore and O. Sporns, Complex brain networks: Graph theoretical analysis of structural and functional systems, *Nat. Rev. Neurosci.* **10**, 186 (2009).
- [13] R. Albert and A. L. Barabási, Statistical mechanics of complex networks, *Nat. Rev. Neurosci.* **74**, 47 (2002).
- [14] S. Dorogovtsev, A. Goltsev, and J. F. Mendes, Critical phenomena in complex networks, *Rev. Mod. Phys.* **80**, 1275 (2008).
- [15] J. A. Holyst, K. Kacperski, and F. Schweitzer, Phase transitions in social impact models of opinion formation, *Physica A* **285**, 199 (2000).
- [16] D. Tsarev, A. Trofimova, A. Alodjants, and A. Khrennikov, Phase transitions, collective emotions and decision-making problem in heterogeneous social systems, *Sci. Rep.* **9**, 18039 (2019).
- [17] T. Pham, I. Kondor, R. Hanel, and S. Thurner, The effect of social balance on social fragmentation, *J. R. Soc. Interface* **17**, 20200752 (2020).
- [18] M. Leone, A. Vazquez, F. Vespignani, and R. Zecchina, Ferromagnetic ordering in graphs with arbitrary degree distribution, *Eur. Phys. J. B* **28**, 191 (2002).
- [19] G. Bianconi, Enhancement of t_c in the superconductor-insulator phase transition on scale-free networks, *J. Stat. Mech.* (2012) P07021.
- [20] M. Krasnytska, B. Berche, Y. Holovatch, and R. Kenna, Partition function zeros for the Ising model on complete graphs and on annealed scale-free networks, *Phys. A: Math. Theor.* **49**, 135001 (2016).
- [21] G. Bianconi and A. L. Barabási, Bose-Einstein Condensation in Complex Networks, *Phys. Rev. Lett.* **86**, 5632 (2001).
- [22] G. Bianconi, Mean field solution of the Ising model on a Barabási-Albert network, *Phys. Lett. A* **303**, 166 (2002).
- [23] K. Suchecki and J. A. Holyst, Order, disorder and criticality: Advanced problems of phase transition theory, World Scientific Publishing **3**, 167 (2013).
- [24] S. N. Dorogovtsev, A. V. Goltsev, and J. F. F. Mendes, Ising model on networks with an arbitrary distribution of connections, *Phys. Rev. E* **66**, 016104 (2002).
- [25] A. Aleksiejuk, J. A. Holyst, and D. Stauffer, Ferromagnetic phase transition in Barabási-Albert networks, *Physica A* **310**, 260 (2002).
- [26] J. Krishnan, R. Torabi, E. Di Napoli, C. Honerkamp, and A. Schuppert, Long-range Ising model of a Barabási-Albert network, [arXiv:2005.05045](https://arxiv.org/abs/2005.05045).
- [27] S. Suzuki, J. I. Inoue, and B. K. Chakrabarti, *Quantum Ising Phases and Transitions in Transverse Ising Models*, Vol. 862 (Springer, Heidelberg, New York, Dordrecht, London, 2012), p. 403.
- [28] I. Buluta, S. Ashhab, and N. Franco, Natural and artificial atoms for quantum computation, *Rep. Prog. Phys.* **74**, 104401 (2011).
- [29] K. Hepp and E. H. Lieb, Equilibrium statistical mechanics of matter interacting with the quantized radiation field, *Phys. Rev. A* **8**, 2517 (1973).
- [30] Y. K. Wang and F. T. Hioe, Phase transition in the Dicke model of superradiance, *Phys. Rev. A* **7**, 831 (1973).
- [31] C. Emary and T. Brandes, Chaos and the quantum phase transition in the Dicke model, *Phys. Rev. E* **67**, 066203 (2003).
- [32] J. Larson and E. K. Irish, Some remarks on ‘superradiant’ phase transitions in light-matter systems, *J. Phys. A: Math. Theor.* **50**, 174002 (2017).
- [33] J. G. Bohnet, Z. Chen, M. D. Weiner, J. M., M. J. Holland, and J. K. Thompson, A steady-state superradiant laser with less than one intracavity photon, *Nature* **484**, 7392 (2017).

- [34] I. Y. Chestnov, A. P. Alodjants, and S. M. Arakelian, Lasing and high-temperature phase transitions in atomic systems with dressed-state polaritons, *Phys. Rev. A* **88**, 063834 (2013).
- [35] E. Akkermans, A. Gero, and R. Kaiser, Photon Localization and Dicke Superradiance in Atomic Gases, *Phys. Rev. Lett.* **101**, 103602 (2008).
- [36] P. R. Eastham and P. B. Littlewood, Bose condensation of cavity polaritons beyond the linear regime: The thermal equilibrium of a model microcavity, *Phys. Rev. B* **64**, 235101 (2001).
- [37] Z. Wang, H. F. W. Li, X. Song, C. Song, W. Liu, and H. Wang, Controllable Switching Between Superradiant and Subradiant States in a 10-Qubit Superconducting Circuit, *Phys. Rev. Lett.* **124**, 013601 (2020).
- [38] M. Bamba, K. Inomata, and Y. Nakamura, Superradiant Phase Transition in a Superconducting Circuit in Thermal Equilibrium, *Phys. Rev. Lett.* **117**, 173601 (2016).
- [39] K. Cong, Q. Zhang, Y. Wang, G. T. Noe, A. Belyanin, and J. Kono, Dicke superradiance in solids, *J. Opt. Soc. Am. B* **33**, 80 (2016).
- [40] S. Yalouz and V. Pouthier, Continuous-time quantum walk on an extended star graph: Trapping and superradiance transition, *Phys. Rev. E* **97**, 022304 (2018).
- [41] K. Vahala, Optical microcavities, *Nature* **424**, 839 (2003).
- [42] A. Alodjants, I. Barinov, and S. Arakelian, Strongly localized polaritons in an array of trapped two-level atoms interacting with a light field, *J. Phys. B: At., Mol. Opt. Phys.* **43**, 095502 (2010).
- [43] H. Deng, H. Haug, and Y. Yamamoto, Exciton-polariton Bose-Einstein condensation, *Rev. Mod. Phys.* **82**, 1489 (2010).
- [44] I. Chestnov, A. Alodjants, S. Arakelian, J. Klaers, F. Vewinger, and M. Weitz, Bose-Einstein condensation for trapped atomic polaritons in a biconical waveguide cavity, *Phys. Rev. A* **85**, 053648 (2012).
- [45] O. Berman, Y. Lozovik, and D. Snoke, Theory of Bose-Einstein condensation and superfluidity of two-dimensional polaritons in an in-plane harmonic potential, *Phys. Rev. B* **77**, 155317 (2008).
- [46] S. Gammelmark and K. Mølmer, Phase transitions and heisenberg limited metrology in an Ising chain interacting with a single-mode cavity field, *New J. Phys.* **13**, 053035 (2011).
- [47] C. F. Lee and N. F. Johnson, First-Order Superradiant Phase Transitions in a Multiqubit Cavity System, *Phys. Rev. Lett.* **93**, 083001 (2004).
- [48] A. Y. Bazhenov, D. V. Tsarev, and A. P. Alodjants, Temperature quantum sensor on superradiant phase-transition, *Physica B* **579**, 411879 (2020).
- [49] A. Khrennikov, Social laser: Action amplification by stimulated emission of social energy, *Philos. Trans. R. Soc. A* **374**, 20150094 (2016).
- [50] A. Khrennikov, Z. Toffano, and F. Dubois, Concept of information laser: From quantum theory to behavioural dynamics, *Eur. Phys. J.: Spec. Top.* **227**, 2133 (2019).
- [51] W. Cota, S. Ferreira, and R. Pastor-Satorras, Quantifying echo chamber effects in information spreading over political communication networks, *EPJ Data Sci.* **8**, 35 (2019).
- [52] F. Baumann, P. Lorenz-Spreen, I. Sokolov, and M. Starnini, Modeling Echo Chambers and Polarization Dynamics in Social Networks, *Phys. Rev. Lett.* **124**, 048301 (2020).
- [53] V. Guleva, E. Shikov, K. Bochenina, S. Kovalchuk, A. Alodjants, and A. Boukhanovsky, Emerging complexity in distributed intelligent systems, *Entropy* **22**, 1437 (2020).
- [54] S. H. Lee, M. Ha, H. Jeong, J. D. Noh, and H. Park, Critical behavior of the Ising model in annealed scale-free networks, *Phys. Rev. E* **80**, 051127 (2009).
- [55] E. Lifshitz and L. Pitaevskii, *Statistical Physics: Theory of the Condensed State, Part 2* (Elsevier, Amsterdam, 2013), p. 38.
- [56] D. Snoke, Polariton condensation and lasing, in *Exciton Polaritons in Microcavities*, Springer Series in Solid-State Sciences, edited by V. Timofeev and D. Sanvitto (Springer, Berlin, 2012), Vol. 172, 307.
- [57] Y.-Y. Liu, J. Slotine, and A. Barabasi, Controllability of complex networks, *Nature* **473**, 167 (2011).